

AsCL: An Asymmetry-sensitive Contrastive Learning Method for Image-Text Retrieval with Cross-Modal Fusion

1st Ziyu Gong

State Key Laboratory for
Novel Software Technology
Nanjing University
Nanjing, China
ziyugong@smail.nju.edu.cn

2nd Chengcheng Mai

School of Computer Science and Electronic Information/
School of Artificial Intelligence
Nanjing Normal University
Nanjing, China
maicc@nju.edu.cn

3rd Yihua Huang*

State Key Laboratory for
Novel Software Technology
Nanjing University
Nanjing, China
yhuang@nju.edu.cn

Abstract—The image-text retrieval task aims to retrieve relevant information from a given image or text. The main challenge is to unify multimodal representation and distinguish fine-grained differences across modalities, thereby finding similar contents and filtering irrelevant contents. However, existing methods mainly focus on unified semantic representation and concept alignment for multi-modalities, while the fine-grained differences across modalities have rarely been studied before, making it difficult to solve the information asymmetry problem. In this paper, we propose a novel asymmetry-sensitive contrastive learning method. By generating corresponding positive and negative samples for different asymmetry types, our method can simultaneously ensure fine-grained semantic differentiation and unified semantic representation between multi-modalities. Additionally, a hierarchical cross-modal fusion method is proposed, which integrates global and local-level features through a multimodal attention mechanism to achieve concept alignment. Extensive experiments performed on MSCOCO and Flickr30K, demonstrate the effectiveness and superiority of our proposed method.

Index Terms—Image-text Retrieval, Information Asymmetry, Contrastive Learning, Cross-modal Fusion

I. INTRODUCTION

Image-text retrieval aims to search for relevant text based on visual queries and vice versa. Early efforts contribute significantly to the learning of unified multimodal representation and visual-textual concept alignment, but it still faces the following challenge: the existing work rarely considers the problem of cross-modal information asymmetry, which neglects the fine-grained differences between modalities.

The information asymmetry problem in the multimodal retrieval task refers to the unequal information capacity between different modalities, *i.e.*, when describing the same scene, one modality may contain more or less information than the other modality. Image modality objectively describes the scene based on pixels, while text modality describes the scene based on characters or words. It should be noted that different modalities have different emphases on the description of a certain scene. For a certain image, the paired text may be partially similar to the image and partially different from the image. The information asymmetry problem aggravates the

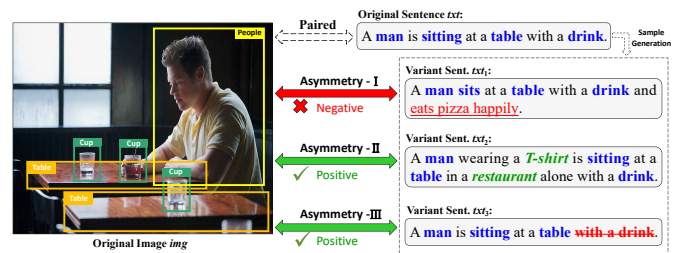


Fig. 1. Fine-grained information asymmetry types.

difficulty of the image-text retrieval task. As shown in Figure 1, for a given paired image-text pair, (img, txt) , we subdivided information asymmetry into three types. (1) Asymmetry-I: The text contains redundant information that does not exist in the image. For variant txt_1 , although txt_1 contains most of the objects corresponding to image img , such as “people”, “table”, and “cup”, txt_1 mistakenly contains “pizza” that is not mentioned in image. Therefore, txt_1 should be considered a negative of img . However, existing models would mistakenly retrieve txt_1 as a positive because it contains most of the information in the image. (2) Asymmetry-II: Compared to the original paired text, the variant text contains more relevant information belonging to the corresponding image. For variant txt_2 , it is a more informative illustration of img , which contains more details about clothing and location without irrelevant content, and should be regarded as a positive of img . (3) Asymmetry-III: Compared to the original paired text, the variant text discards partial information contained in the given image, but still conforms to the description of the image. For variant txt_3 , although the word “drink” has been deleted, it should still be considered a positive of img as it fits the description of img . However, existing models may mistakenly identify it as a negative or lower its retrieval ranking because the proportion of overlapping concepts between txt_3 and img has decreased.

To address the above issues, a novel asymmetry-sensitive

contrastive learning method was presented. For each fine-grained information asymmetry type, we generated corresponding positive or negative textual samples with both partially similar parts and subtly different parts, which can be leveraged in the optimization of contrastive learning and acquire more discriminative multimodal semantic representations. In particular, for Asymmetry-I, we generated negative samples by adding noise information into the embedding layer to fully enhance the diversity of the generated negatives. For Asymmetry-II and Asymmetry-III, we generated positive samples by concatenating and truncating keywords on the original input statements, respectively, in order to enrich the diversity of semantic descriptions for the same scenario.

Our method enhanced the sensitivity of the contrastive learning algorithm to the fine-grained information asymmetry across modalities by increasing the diversity of positive and negative samples, and provided semantic representation support for the subsequent multimodal retrieval task based on semantic similarity. In addition, in order to capture more sophisticated correlations across modalities, a hierarchical cross-modal fusion has also been proposed, for achieving multimodal concept alignment at both image-text and region-word levels, through a cross-modal attention mechanism.

The major contributions can be concluded as follows: (1) An asymmetry-sensitive contrastive learning method was proposed to solve the fine-grained information asymmetry problem between images and texts, where corresponding positives and negatives for each asymmetry type are generated to achieve unified semantic representation for better cross-modality retrieval based on semantic similarity. (2) We also presented an image-text feature fusion and semantic alignment method based on a cross-modal attention mechanism for high-quality modality interaction, from both global and local perspectives. (3) Extensive experiments verified that our method outperformed the state-of-the-art baselines.

II. OUR ASCL METHODOLOGY

A. Multi-modal Feature Representation

As shown in Figure 2, for each input image, we extracted K region features with the pretrained Faster-RCNN model and then projected them into a D -dimensional space, denoted as $\mathbf{V} = [\mathbf{v}_1, \mathbf{v}_2, \dots, \mathbf{v}_K] \in \mathbb{R}^{K \times D}$. Meanwhile, we acquired the global feature with the pretrained ResNet152 model and then transformed it into a D -dimensional vector, *i.e.*, $\mathbf{G} \in \mathbb{R}^D$.

For each input text, we utilized BERT to obtain word embeddings, $\mathbf{W} = [\mathbf{w}_1, \mathbf{w}_2, \dots, \mathbf{w}_L] \in \mathbb{R}^{L \times D}$, where L is the number of words and D is the dimension of word features.

B. Information Asymmetry and Sample Generation

Information asymmetry quantifies the differences between the sets of image and text information. According to fine-grained information asymmetries, we generated different samples. **Asymmetry-I:** The text contains more redundant information that does not belong to the corresponding image. We used four methods to generate diverse negative samples by adding noise information to the textual embedding layers:

- (i) Gaussian Noise: Gaussian noise is random variation that follows a Gaussian (normal) distribution. We directly attached it to \mathbf{W} .
 - (ii) Token Shuffling: The order of tokens in \mathbf{W} was randomly altered.
 - (iii) Token Cutoff & Feature Cutoff: We assigned zero to a row (token) or a column (feature) of \mathbf{W} .
 - (iv) Dropout: We randomly discarded elements in \mathbf{W} based on a specific probability.
- Asymmetry-II:** The text contains more relevant information that belongs to the corresponding image. For each image in the original dataset, there are five corresponding captions sharing similar concepts. We generated a long positive sentence by randomly selecting two related sentences and concatenating them into the long sentence.
- Asymmetry-III:** The text discards partial relevant information that belongs to the corresponding image. We truncated the original text to generate a short but positive sentence, which increases the diversity of positives.

C. Cross-modal Fusion

Local Region-Word Fusion. Due to the bidirectional requirement of image-text retrieval, we defined $\mathbf{X} = [\mathbf{x}_1, \mathbf{x}_2, \dots, \mathbf{x}_M] \in \mathbb{R}^{M \times D}$ and $\mathbf{Y} = [\mathbf{y}_1, \mathbf{y}_2, \dots, \mathbf{y}_N] \in \mathbb{R}^{N \times D}$ to denote the given query (image or text) and the retrieved results (text or image), respectively, where $\mathbf{x}_i \in \mathbb{R}^D$ and $\mathbf{y}_i \in \mathbb{R}^D$ are represented as region-level or word-level features. In this work, we implemented two single symmetrical versions of formula. Hence, we set $\mathbf{X} := \mathbf{V}(M := K)$ and $\mathbf{Y} := \mathbf{W}(N := L)$ for the image-to-text (I2T) version, and $\mathbf{X} := \mathbf{W}(M := L)$ and $\mathbf{Y} := \mathbf{V}(N := K)$ for the text-to-image (T2I) version. “:=” is an assignment operator. $\mathbf{V} \in \mathbb{R}^{K \times D}$, $\mathbf{W} \in \mathbb{R}^{L \times D}$ are defined in Section 2.1, and will be assigned to \mathbf{X} or \mathbf{Y} in different retrieval versions.

Instead of treating all region-word pairs equally, a multi-head cross-modal attention mechanism was adopted to allocate weights to regions and words based on their contribution.

$$\begin{aligned} \mathbf{Y}^* &= \text{MultiHead}(\text{Query} := \mathbf{X}, \text{Key} := \mathbf{Y}, \text{Value} := \mathbf{Y}) \\ &= \text{Concat}(\text{head}_1, \dots, \text{head}_i, \dots, \text{head}_H) \mathbf{Z}^O \end{aligned} \quad (1)$$

where $\mathbf{Y}^* \in \mathbb{R}^{M \times D}$, $\mathbf{Z}^O \in \mathbb{R}^{D \times D}$, H is the number of attention heads, and $\text{Concat}(\cdot)$ represents the concatenation operation across the feature dimension D . In this work, $\text{head}_i = \text{Att}(\text{Query}_i := \mathbf{X} \mathbf{Z}_i^X, \text{Key}_i := \mathbf{Y} \mathbf{Z}_i^Y, \text{Value}_i := \mathbf{Y} \mathbf{Z}_i^Y)$, where Att refers to the scaled dot-product attention, and $\mathbf{Z}_i^X, \mathbf{Z}_i^Y \in \mathbb{R}^{D \times \frac{D}{H}}$.

For I2T, the output \mathbf{Y}^* denotes the region-attended text representations $\mathbf{W}^* = [\mathbf{w}_1^*, \mathbf{w}_2^*, \dots, \mathbf{w}_K^*] \in \mathbb{R}^{K \times D}$ for each region, while for T2I, it refers to the word-attended image representations $\mathbf{V}^* = [\mathbf{v}_1^*, \mathbf{v}_2^*, \dots, \mathbf{v}_L^*] \in \mathbb{R}^{L \times D}$ for each word. Here, $\mathbf{w}_i^* \in \mathbb{R}^D$ represents the region-attended text representation for the i -th region, and $\mathbf{v}_i^* \in \mathbb{R}^D$ represents the word-attended image representation for the i -th word.

Global Image-Text Fusion. To further capture complex cross-modal correlation, we jointly mapped holistic images and sentences into a common space for global semantic consistence and heterogeneity minimization. To be specific, for the region-attended text representations \mathbf{W}^* obtained in

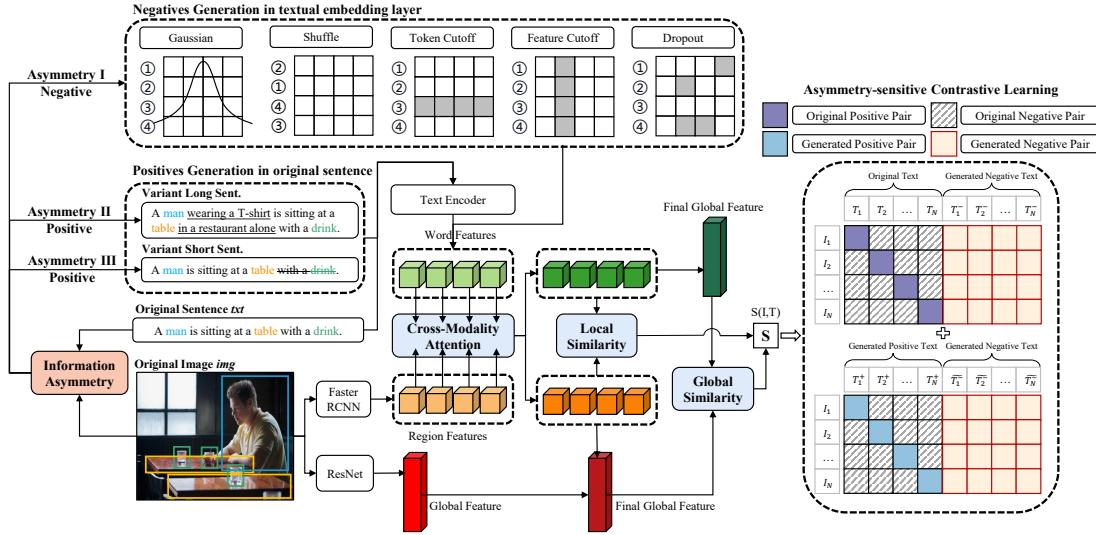


Fig. 2. The overview of our proposed AsCL Method.

the process of local fusion, we first computed its average vector (denoted as $\bar{\mathbf{W}}^* = \frac{\sum_{i=0}^K \mathbf{w}_i^*}{K}$), and then projected it into a common space. The output result is $\mathbf{W}_g = \mathbf{X}_w^T \bar{\mathbf{W}}^*$, which serves as the final global representation of text, and \mathbf{X}_w is a learnable embedding matrix. Similarly, we separately projected the average vector of \mathbf{V}^* (represented as $\bar{\mathbf{V}}^* = \frac{\sum_{i=0}^L \mathbf{v}_i^*}{L}$) and the feature vector of the entire image (represented as \mathbf{G}) into the common embedding space as $\mathbf{V}_{g_1} = \mathbf{X}_v^T \bar{\mathbf{V}}^*$ and $\mathbf{V}_{g_2} = \mathbf{X}_g^T \mathbf{G}$. \mathbf{X}_v and \mathbf{X}_g are all learnable embedding matrices. The final global representation of image can be fused as $\mathbf{V}_g = \text{Fusion}(\mathbf{V}_{g_1}, \mathbf{V}_{g_2})$.

D. AsCL for I-T Matching

The matching score between image I and text T consists of two components: local similarity score and global similarity score. According to the region-attended text representations \mathbf{W}^* and the word-attended image representations \mathbf{V}^* , the local matching score is formulated as,

$$S_{local}(I, T) = \frac{\sum_{i=1}^k R(\mathbf{v}_i, \mathbf{w}_i^*)}{2K} + \frac{\sum_{j=1}^L R(\mathbf{w}_j, \mathbf{v}_j^*)}{2L} \quad (2)$$

, where $R(\mathbf{x}, \mathbf{y}) = \frac{\mathbf{x}^T \mathbf{y}}{\|\mathbf{x}\| \cdot \|\mathbf{y}\|}$. Meanwhile, the global matching score between image I and text T is represented as:

$$S_{global}(I, T) = R(\mathbf{V}_g, \mathbf{W}_g). \quad (3)$$

Based on the local and global matching scores, the similarity score between image I and text T can be defined as:

$$S(I, T) = u_1 \cdot S_{local}(I, T) + (1 - u_1) \cdot S_{global}(I, T) \quad (4)$$

where u_1 is a hyper-parameter.

On this basis, we proposed a novel asymmetry-sensitive contrastive learning method by exploiting the generated positives and negatives according to our defined asymmetry types.

I-T Matching for Asymmetry-I. During training, there are N image-text pairs in a batch. According to our defined

Asymmetry-I, we generated N negative sentences by adding noise. For each positive pair (I, T) , we retrieved $N-1$ in-batch negative images $\{\hat{I}_n\}_{n=1}^{N-1}$, $N-1$ in-batch negative sentences $\{\hat{T}_n\}_{n=1}^{N-1}$, and especially N generated negative sentences $\{T_n^-\}_{n=1}^N$ for Asymmetry-I. Therefore, the objective function for Asymmetry-I can be formulated as follows:

$$L_I(I, T) = \frac{e^{S(I, T)/\tau}}{e^{S(I, T)/\tau} + \sum_{n=1}^{N-1} e^{S(\hat{I}_n, T)/\tau}} + \frac{e^{S(I, T)/\tau}}{e^{S(I, T)/\tau} + \sum_{n=1}^{N-1} e^{S(I, \hat{T}_n)/\tau} + \sum_{n=1}^N \alpha_n \cdot e^{S(I, T_n^-)/\tau}} \quad (5)$$

where α_n is set to zero if the similarity score of the image-text pair exceeds the positive pair, otherwise we set α_n to 1.

I-T Matching for Asymmetry-II&III. For each positive image-text pair (I, T) , we generated the content-variant long sentence or short sentence as another positive sample, T^+ , according to our defined Asymmetry-II and Asymmetry-III. Here, (I, T^+) is a newly generated positive pair, while T^+ is also considered as a negative sample for other images in the same batch. Likewise, we added noise information to textual representations of these generated positives as additional negative samples. Consequently, there exist $N-1$ in-batch negative images $\{\hat{I}_n\}_{n=1}^{N-1}$, $N-1$ in-batch negative sentences $\{\hat{T}_n^+\}_{n=1}^{N-1}$, and N generated negative sentences $\{\hat{T}_n^-\}_{n=1}^N$ towards every positive pair (I, T^+) . For Asymmetry-II & III, T^+ plays a similar role in Equation 6 as T in Equation 5.

$$L_{II\&III}(I, T^+) = \frac{e^{S(I, T^+)/\tau}}{e^{S(I, T^+)/\tau} + \sum_{n=1}^{N-1} e^{S(\hat{I}_n, T^+)/\tau}} + \frac{e^{S(I, T^+)/\tau}}{e^{S(I, T^+)/\tau} + \sum_{n=1}^{N-1} e^{S(I, \hat{T}_n^+)/\tau} + \sum_{n=1}^N \alpha_n \cdot e^{S(I, \hat{T}_n^-)/\tau}} \quad (6)$$

Overall Training. The overall training of AsCL for all types of information asymmetry is shown as follows:

$$L_{AsCL}(I, T) = \frac{1}{2}L_I(I, T) + \frac{1}{2}L_{II\&III}(I, T^+) \quad (7)$$

III. EXPERIMENTS AND ANALYSES

A. Experimental Settings

Dataset. We conducted experiments on two benchmark datasets: MSCOCO [1] and Flickr30K [2]. (1) MSCOCO: It consists of a train split of 113,287 images, a validation split of 5,000 images, and a test split of 5,000 images. Each image is annotated with 5 sentences. We adopted the evaluation setting MSCOCO (5K), *i.e.*, directly testing on the full 5K images. (2) Flickr30K: It contains 31,783 images, each with 5 corresponding sentences. It was split into 29,783 training images, 1,000 validation images and 1,000 testing images.

Implementation Details. We adopted R@K(K=1,5,10) to evaluate performance, which measures the percentage of ground truth being retrieved among top-K results. Higher R@K indicates better performance. We optimized AsCL on one NVIDIA Tesla A100 using PyTorch library. The Adam optimizer was employed with a batch size 64 and 20 epochs. We set the dimension of joint embedding space D to 1024, the number of regions K to 36. For MSCOCO, the learning rate was set to $5e-4$ with decaying 10% of every 10 epochs, τ was set to 0.05 and u_1 was set to 0.8. For Flickr30K, the learning rate was set to $2e-4$ at first and declined by ten times every 10 epochs, τ was set to 0.01 and u_1 was set to 0.6.

B. Image-Text Retrieval Results

As shown in Table I, our method outperformed existing state-of-art baselines across two benchmark datasets for the image-text retrieval task. For MSCOCO (5K), compared with LexLIP [3], our model achieved a huge improvement of 24.6% (94.8% vs. 70.2%) in terms of I2T/R@1 and 13.5% (66.7% vs. 53.2%) in terms of T2I/R@1. For Flickr30K (1K), our model outperformed LexLIP by 7.7% (99.1% vs. 91.4%) on I2T/R@1 and 4.6% (83.0% vs. 78.4%) on T2I/R@1. Overall, according to fine-grained information asymmetry types, AsCL exhibits great effectiveness and superiority for the image-text retrieval task by leveraging corresponding generated samples.

C. Ablation Experiments and Results

Different Samples. We compared three variant models with different generated samples according to different asymmetry types: (1) “-w/o Pos.”: We only generated negative sentences for Asymmetry-I. (2) “-w/o Neg.”: We only generated positive sentences for Asymmetry-II and Asymmetry-III. (3) “-w/o P&N.”: We did not generate additional samples. As shown in Table II, after removing generated positives, generated negatives and all generated samples, the results on Flickr30K (1K) decreased gradually, from 99.1% to 98.8% on I2T/R@1, from 99.8% to 99.4% on I2T/R@5, from 83.0% to 76.4% on T2I/R@1 and from 95.4% to 91.5% on T2I/R@5. Similar

results can be observed on the MSCOCO (5K). The performance degradation verified the necessity of generated samples instantiated from different asymmetry types.

We delved into more fine-grained sample generation strategies for each asymmetry type. The generation of negatives employs five noise addition strategies for Asymmetry-I, including “Shuffle”, “Dropout”, “Gaussian”, “Cutoff” and “Mixture”. The generation of positives involves two strategies, concatenation for Asymmetry-II and truncation for Asymmetry-III. As illustrated in Figure 3, we found that: (1) The short text for Asymmetry-III outperformed the generated long text for Asymmetry-II. We argued that although overlapping concepts between the short text and the given image has been reduced, the short text for Asymmetry-III should still be considered as a positive sample, which helps provide more diversity perspectives for learning robust semantic representation. (2) The Rsum values of “Shuffle”, “Dropout”, “Gaussian”, and “Cutoff” were all lower than that of “Mixture”. We supposed that “Mixture” enriches the diversity of negative textual descriptions for Asymmetry-I, thereby improving retrieval performance. Rsum is the sum of R@1+R@5+R@10 in both I2T and T2I. Higher Rsum means better performance.

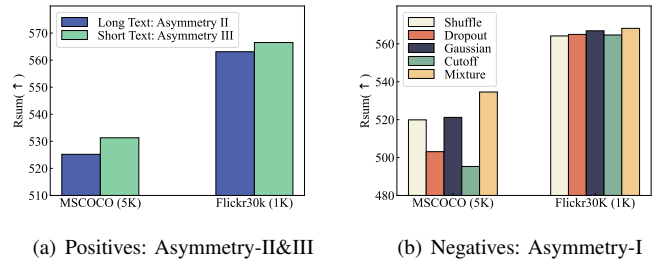


Fig. 3. Performance comparison of diverse samples based on fine-grained generation strategies for each asymmetry type. (a) Influence of different generated positives according to Asymmetry-II and Asymmetry-III. (b) Influence of generated negatives with different noise addition strategies according to Asymmetry-I. \uparrow means higher, better.

Cross-modal Fusion. After removing cross-modal fusion (denoted as “-w/o MF” in Table II), all metrics on two datasets dramatically decreased, indicating that the hierarchical modal fusion via multi-head attention mechanism helps discover latent alignment from both global and local perspectives.

Objective Function. Compared to AsCL, the performance of triplet loss (denoted as “-w triplet loss” in Table II) declined, with R@1/I2T from 94.8 to 89.4 and R@1/I2T from 66.7 to 58.6 on MSCOCO (5K), which verified the superiority of our proposed asymmetry-sensitive contrastive learning.

D. Alignment and Uniformity Experiments and Results

Alignment and uniformity are two key properties related to the quality of contrastive learning, which play an important role in the task of image-text retrieval.

Alignment Evaluation. Alignment prefers a closer distance between positive pairs. Positive pairs consists of two parts: inter-modal image-text pairs and intra-modal text-text

TABLE I

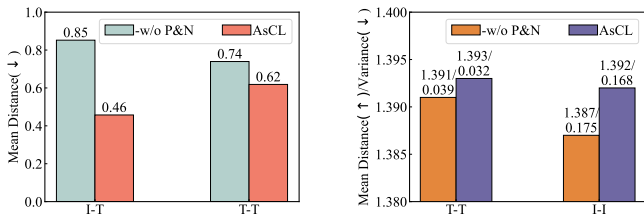
COMPARISON RESULTS OF THE IMAGE-TEXT RETRIEVAL ON MSCOCO (5K TEST SET) AND FLICKR30K (1K TEST SET). WE CONDUCTED EXPERIMENTS 5 TIMES AND REPORTED THE AVERAGE VALUE.

| Model | MSCOCO (5K test set) | | | | | | Flickr30K (1K test set) | | | | | |
|--------------------|----------------------|-------------|-------------|-------------|-------------|-------------|-------------------------|-------------|------------|-------------|-------------|-------------|
| | I2T | | | T2I | | | I2T | | | T2I | | |
| | R@1 | R@5 | R@10 | R@1 | R@5 | R@10 | R@1 | R@5 | R@10 | R@1 | R@5 | R@10 |
| VSE++ [4] | 41.3 | 71.1 | 81.2 | 30.3 | 59.4 | 72.4 | 52.9 | 80.5 | 87.2 | 39.6 | 70.1 | 79.5 |
| SCAN [5] | 50.4 | 82.2 | 90.0 | 38.6 | 69.3 | 80.4 | 67.4 | 90.3 | 95.8 | 48.6 | 77.7 | 85.2 |
| IMRAM [6] | 53.7 | 83.2 | 91.0 | 39.6 | 69.1 | 79.8 | 74.1 | 93.0 | 96.6 | 53.9 | 79.4 | 87.2 |
| DIME [7] | 59.3 | 85.4 | 91.9 | 43.1 | 73.0 | 83.1 | 81.0 | 95.9 | 98.4 | 63.6 | 88.1 | 93.0 |
| DSRAN [8] | 57.9 | 85.3 | 92.0 | 41.7 | 72.7 | 82.8 | 80.5 | 95.5 | 97.9 | 59.2 | 86.0 | 91.9 |
| TAGS-DC [9] | 67.8 | 89.6 | 94.2 | 53.3 | 80.0 | 88.0 | 90.6 | 98.8 | 99.1 | 77.3 | 94.3 | 97.3 |
| UNITER+DG [10] | 51.4 | 78.7 | 87.0 | 39.1 | 68.0 | 78.3 | 78.2 | 93.0 | 95.9 | 66.4 | 88.2 | 92.2 |
| SOHO [11] | 66.4 | 88.2 | 93.8 | 50.6 | 78.0 | 86.7 | 86.5 | 98.1 | 99.3 | 72.5 | 92.7 | 96.1 |
| ViSTA [12] | 68.9 | 90.1 | 95.4 | 52.6 | 79.6 | 87.6 | 89.5 | 98.4 | 99.6 | 75.8 | 94.2 | 96.9 |
| COTS [13] | 69.0 | 90.4 | 94.9 | 52.4 | 79.0 | 86.9 | 90.6 | 98.7 | 99.7 | 76.5 | 93.9 | 96.6 |
| LightningDoT [14] | 64.6 | 87.6 | 93.5 | 50.3 | 78.7 | 87.5 | 86.5 | 97.5 | 98.9 | 72.6 | 93.1 | 96.1 |
| LexLIP [3] | 70.2 | 90.7 | 95.2 | 53.2 | 79.1 | 86.7 | 91.4 | 99.2 | 99.7 | 78.4 | 94.6 | 97.1 |
| AsCL (OURS) | 94.8 | 99.4 | 99.8 | 66.7 | 87.3 | 92.3 | 99.1 | 99.8 | 100 | 83.0 | 95.4 | 97.6 |

TABLE II
ABLATION RESULTS ON MSCOCO AND FLICKR30K.

| Model Variants | MSCOCO (5K) | | | | Flickr30K (1K) | | | |
|-----------------|-------------|------|------|------|----------------|------|------|------|
| | I2T | | T2I | | I2T | | T2I | |
| | R@1 | R@5 | R@1 | R@5 | R@1 | R@5 | R@1 | R@5 |
| AsCL | 94.8 | 99.4 | 66.7 | 87.3 | 99.1 | 99.8 | 83.0 | 95.4 |
| -w/o Pos. | 93.1 | 99.1 | 65.1 | 86.0 | 99.0 | 99.7 | 79.6 | 92.7 |
| -w/o Neg. | 94.8 | 99.3 | 61.2 | 83.3 | 98.8 | 99.6 | 77.2 | 91.9 |
| -w/o P&N | 93.1 | 98.8 | 59.1 | 81.6 | 98.8 | 99.4 | 76.4 | 91.5 |
| -w/o MF | 39.7 | 71.2 | 31.0 | 58.7 | 77.5 | 95.9 | 47.0 | 71.3 |
| -w triplet loss | 89.4 | 99.8 | 58.6 | 79.8 | 98.3 | 99.2 | 73.3 | 87.9 |

pairs. We separately calculated the average Euclidean distance between positive pairs in MSCOCO (5K) under our model AsCL and the ablated model $AsCL_{-w/o P\&N}$. As shown in Figure 4(a), compared with representations learned from model $AsCL_{-w/o P\&N}$, both the average distance between positive image-text (I-T) pairs and the average distance between positive text-text (T-T) pairs learned from AsCL decreased. These results indicated that our method acquired high-quality semantic representations, thereby achieving better inter-modality and intra-modality semantic alignment.



(a) Alignment: Positives get close. (b) Uniformity: Negatives get apart.

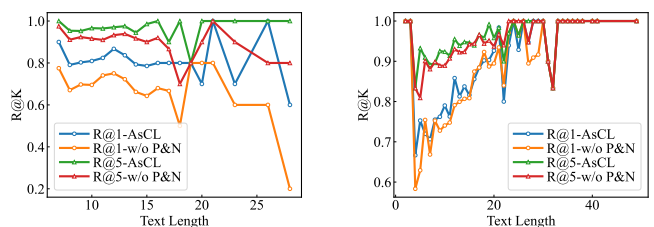
Fig. 4. Mean distance between positive pairs(a) and negative pairs(b) in high-dimensional space on MSCOCO. ↑ means higher, better. ↓ means lower, better.

Uniformity Evaluation. Uniformity favors a uniform distribution of feature embeddings on a hypersphere. We calculated the average Euclidean distance among all images and all texts with different semantics in MSCOCO (5K), respectively. In

Figure 4(b), compared with model $AsCL_{-w/o P\&N}$, the average spacing among different texts under AsCL enlarged (1.393 vs 1.391), along with the drop of variance (0.032 vs 0.039). The average distance and variance between different images exhibited similar phenomenon. It indicated that representations learned from AsCL are more widely and evenly distributed, which verified better uniformity.

E. Impact on Text Queries with Different Lengths

We further conducted text-to-image(T2I) task based on textual queries with different text lengths. We sampled 1,000 sentences from MSCOCO and Flickr30K, respectively. From Figure 5, for those textual queries (especially less than 10 words), AsCL yielded better image retrieval results. One possible explanation is that we generated short sentences as positive samples based on Asymmetry-III during training, which makes AsCL more sensitive and effective to short sentences.



(a) Image Retrieval in MSCOCO. (b) Image Retrieval in Flickr30K.

Fig. 5. Image retrieval for text queries of different lengths.

IV. RELATED WORK

Previous work for image-text retrieval mainly focused on unified representation and cross-modal interaction. These methods can be categorized into two types: (1) dual encoder [4], [8], [15], [16], where images and text are separately encoded into a common embedding space by two individual encoders; (2) cross encoder [17]–[19], where images and

texts are jointly encoded by a cross encoder architecture, incorporating two heterogeneous modalities into unified forms.

For the image-text retrieval task, most recent approaches [5], [6], [13] employ contrastive loss with hard negatives, *i.e.*, samples that are more difficult to be distinguished. The optimization process of contrastive loss with hard negatives increases the similarity score of positive image-text pairs while decreasing that of negative pairs, thereby achieving better retrieval performance. Hence, selection strategies for informative samples have been extensively explored. Early works [20], [21] randomly chose negatives from the original dataset for training. Subsequently, based on the generation methods, researchers have incorporated more difficult negatives into contrastive learning. In the UNITER+DG [10] framework, hard negative sentences were sampled based on structure relevance by using a denotation graph. Fan et al. [9] proposed TAGS-DC to generate synthetic sentences automatically as negative samples. Filip Radenovic et al. [22] presented an importance-sampling approach that reweighted negative samples within a batch, aiming to upsample harder negatives in proportion to their difficulty. Based on fine-grained information asymmetry types, our paper proposed an asymmetry-sensitive contrastive learning method with generated positives and negatives for the image-text retrieval task.

V. CONCLUSION

In this paper, we presented a novel asymmetry-sensitive contrastive learning method. Concretely, in order to address fine-grained information asymmetry issues, we generated corresponding positives and negatives for each asymmetry type, which are fully utilized in the optimization of contrastive learning. Our approach enhances sensitivity to subtle differences between two heterogeneous modalities and achieves more discriminative multimodal semantic representations for the subsequent image-text retrieval task. Moreover, from both local and global perspectives, a hierarchical cross-modal fusion module was proposed to capture sophisticated correspondence between visual and semantic modalities through the multimodal attention mechanism. Experimental results on two widely used datasets, *i.e.*, MSCOCO and Flickr30K, have verified that our method outperforms previous state-of-the-art baselines.

ACKNOWLEDGMENT

This work is supported by the National Natural Science Foundation of China (NO. U1811461, 61572250), the Jiangsu Province Science & Technology Research Grant (BE2021729), Key R&D Program Project of Nanjing Jiangbei New Area (ZDYF20200130), and the Collaborative Innovation Center of Novel Software Technology and Industrialization, Jiangsu, China.

REFERENCES

- [1] Tsung-Yi Lin, Michael Maire, Serge Belongie, James Hays, Pietro Perona, Deva Ramanan, Piotr Dollár, and C Lawrence Zitnick, "Microsoft coco: Common objects in context," in *ECCV*. Springer, 2014, pp. 740–755.
- [2] Bryan A Plummer, Liwei Wang, Chris M Cervantes, Juan C Caicedo, Julia Hockenmaier, and Svetlana Lazebnik, "Flickr30k entities: Collecting region-to-phrase correspondences for richer image-to-sentence models," in *ICCV*, 2015, pp. 2641–2649.
- [3] Ziyang Luo, Pu Zhao, Can Xu, Xiubo Geng, Tao Shen, Chongyang Tao, Jing Ma, Qingwei Lin, and Daxin Jiang, "Lexlip: Lexicon-bottlenecked language-image pre-training for large-scale image-text sparse retrieval," in *ICCV*, 2023, pp. 11206–11217.
- [4] Fartash Faghri, David J Fleet, Jamie Ryan Kiros, and Sanja Fidler, "Vse++: Improving visual-semantic embeddings with hard negatives," *BMVC*, 2018.
- [5] Kuang-Huei Lee, Xi Chen, Gang Hua, Houdong Hu, and Xiaodong He, "Stacked cross attention for image-text matching," in *ECCV*, 2018, pp. 201–216.
- [6] Hui Chen, Guiguang Ding, Xudong Liu, Zijia Lin, Ji Liu, and Jungong Han, "Imram: Iterative matching with recurrent attention memory for cross-modal image-text retrieval," in *CVPR*, 2020, pp. 12655–12663.
- [7] Leigang Qu, Meng Liu, Jianlong Wu, Zan Gao, and Liqiang Nie, "Dynamic modality interaction modeling for image-text retrieval," in *SIGIR*, 2021, pp. 1104–1113.
- [8] Keyu Wen, Xiaodong Gu, and Qingrong Cheng, "Learning dual semantic relations with graph attention for image-text matching," *TCSVT*, vol. 31, no. 7, pp. 2866–2879, 2020.
- [9] Zhihao Fan, Zhongyu Wei, Zejun Li, Siyuan Wang, and Jianqing Fan, "Negative sample is negative in its own way: Tailoring negative sentences for image-text retrieval," in *NAACL-HLT*, 2022, pp. 2667–2678.
- [10] Bowen Zhang, Hexiang Hu, Vihan Jain, Eugene Ie, and Fei Sha, "Learning to represent image and text with denotation graph," in *EMNLP*, 2022, pp. 823–839.
- [11] Zhicheng Huang, Zhaoyang Zeng, Yupan Huang, Bei Liu, Dongmei Fu, and Jianlong Fu, "Seeing out of the box: End-to-end pre-training for vision-language representation learning," in *CVPR*, 2021, pp. 12976–12985.
- [12] Mengjun Cheng, Yipeng Sun, Longchao Wang, Xiongwei Zhu, Kun Yao, Jie Chen, Guoli Song, Junyu Han, Jingtuo Liu, Errui Ding, et al., "Vista: vision and scene text aggregation for cross-modal retrieval," in *CVPR*, 2022, pp. 5184–5193.
- [13] Haoyu Lu, Nanyi Fei, Yuqi Huo, Yizhao Gao, Zhiwu Lu, and Ji-Rong Wen, "Cots: Collaborative two-stream vision-language pre-training model for cross-modal retrieval," in *CVPR*, 2022, pp. 15692–15701.
- [14] Siqi Sun, Yen-Chun Chen, Linjie Li, Shuohang Wang, Yuwei Fang, and Jingjing Liu, "Lightningdot: Pre-training visual-semantic embeddings for real-time image-text retrieval," in *NAACL*, 2021, pp. 982–997.
- [15] Jiacheng Chen, Hexiang Hu, Hao Wu, Yuning Jiang, and Changhu Wang, "Learning the best pooling strategy for visual semantic embedding," in *CVPR*, 2021, pp. 15789–15798.
- [16] Antoine Miech, Jean-Baptiste Alayrac, Ivan Laptev, Josef Sivic, and Andrew Zisserman, "Thinking fast and slow: Efficient text-to-visual retrieval with transformers," in *CVPR*, 2021, pp. 9826–9836.
- [17] Xiujuan Li, Xi Yin, Chunyuan Li, Pengchuan Zhang, Xiaowei Hu, Lei Zhang, Lijuan Wang, Houdong Hu, Li Dong, Furu Wei, et al., "Oscar: Object-semantics aligned pre-training for vision-language tasks," in *ECCV*. Springer, 2020, pp. 121–137.
- [18] Jiasen Lu, Dhruv Batra, Devi Parikh, and Stefan Lee, "Vilbert: Pretraining task-agnostic visiolinguistic representations for vision-and-language tasks," *Advances in neural information processing systems*, vol. 32, 2019.
- [19] Yen-Chun Chen, Linjie Li, Licheng Yu, Ahmed El Kholy, Faisal Ahmed, Zhe Gan, Yu Cheng, and Jingjing Liu, "Uniter: Universal image-text representation learning," in *ECCV*. Springer, 2020, pp. 104–120.
- [20] Andrej Karpathy and Li Fei-Fei, "Deep visual-semantic alignments for generating image descriptions," in *CVPR*, 2015, pp. 3128–3137.
- [21] Richard Socher, Andrej Karpathy, Quoc V Le, Christopher D Manning, and Andrew Y Ng, "Grounded compositional semantics for finding and describing images with sentences," *TACL*, vol. 2, pp. 207–218, 2014.
- [22] Filip Radenovic, Abhimanyu Dubey, Abhishek Kadian, Todor Mihaylov, Simon Vandenhende, Yash Patel, Yi Wen, Vignesh Ramanathan, and Dhruv Mahajan, "Filtering, distillation, and hard negatives for vision-language pre-training," in *CVPR*, 2023, pp. 6967–6977.